Performance Analysis of Two-Tier Networks with Closed Access Small-Cells

Gourab Ghatak[†‡], Antonio De Domenico[†], and Marceau Coupechoux[‡]
[†]CEA, LETI, MINATEC, F-38054 Grenoble, France; [‡]LTCI, CNRS, Telecom ParisTech, Université Paris Saclay, France.
Email: gourab.ghatak@cea.fr; antonio.de-domenico@cea.fr, and marceau.coupechoux@telecom-paristech.fr

***Abstract*—The future demands of high data spectral efficiency and ubiquitous coverage are pushing the next generation of cellular networks towards network densification with massive deployments of small cells to complement macro base stations. In this paper, we study a network comprising of closed access small cells along with macro base stations using stochastic geometry. First, the cell association probability is characterized. Additionally, approximate values of the average downlink signal to interference and noise ratio (SINR) and the downlink spectral efficiency are derived. These derivations are carried out without using the classical approach of solving a Laplace functional. For this, the statistical independence of the useful signals and interference powers is exploited. The obtained results can be used to optimize the small cell network deployment and the inter-cell interference coordination functions.**

I. Introduction

To meet the exponentially increasing demands of mobile traffic, operators are evolving their classic macrocell-only networks towards Heterogenous Networks (HetNets) characterized by a dense deployment of small cells [1], thereby bringing the users closer to base stations. In contrast to the macro-cell base station, the small cells have lower power requirements and lower deployment costs. The small cells can be categorized either by their mode of operation: open access, closed access or shared access [2] or by their mode of deployment: co-channel, dedicated channel and hybrid channel [3]. Currently, small cells are deployed in large numbers mainly as home small cells (i.e., femtocells) [1], which are closed/hybrid access small cells providing wireless services to indoor users.

To analyze heterogeneous networks (HetNets), stochastic geometry has gained a lot of interest because of the mathematical tractability of the results and ease of modeling complex and heterogeneous scenarios. ElSawy et. al. [4] recently provided a comprehensive survey on the literature related to stochastic geometry to characterize multi-tier and cognitive wireless networks. The main performance metrics that have been used so far to characterize cellular networks are the coverage probability and the spectral efficiency. To derive these metrics, researchers have used either the Laplace functional of the Poisson point process or the moment generating function (MGF). These approaches are used mainly because the distribution of the aggregate interference is not known in closed form.

Although these methods are mathematically tractable, they are quite calculation intensive to work with. Bai et. al. in [5] used the Laplace functional to derive the coverage probability and rate of a single-tier millimeter wave network whereas in [6], di Renzo et. al. provided an analysis for a multi-tier network using the moment generating function. A multi-tier network comprising of femto and pico cells was analyzed using Poisson cluster process in [7] and the performance metrics of coverage probability and rate were derived using the probability generating functional (PGF) of the cluster processes.

The contributions of this paper is threefold: 1) We provide novel expressions for the small cell and macro cell association probabilities for a user operating in close proximity to its home Small Cell eNode-B (home SCeNB); 2) We provide a new approximate expression for evaluating the average downlink SINR; 3) Based on it, we derive approximations of the average downlink spectral efficiency.

The rest of the paper is organized as follows: we describe the investigated system model with the underlying assumptions in Section II. The results on association probabilities, SINR, and downlink spectral efficiency are presented in Sections III, IV, and V, respectively. Section VI validates the derived results by simulations, and finally the paper concludes in Section VII.

II. System Model

A. Two-Tier Network Model

Consider a two-tier network as shown in Fig. 1 consisting of Macro eNodes-B (MeNB) and SCeNBs. The small cell tier consists of strictly closed access SCeNBs, each providing access to a closed user group.

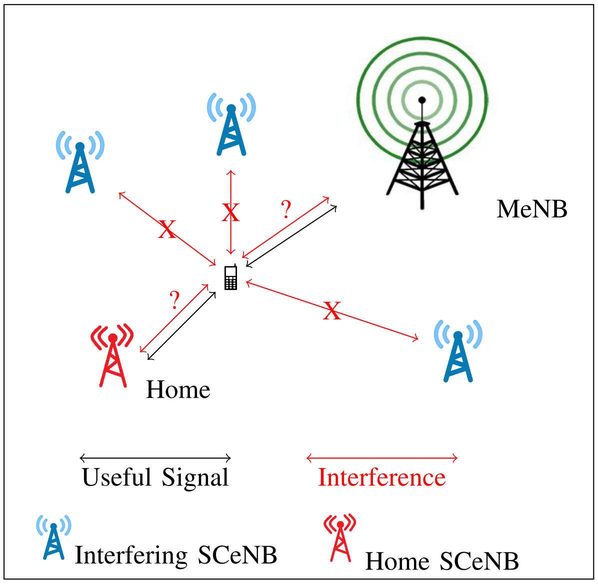

Fig. 1. Deployment of Closed Access SCeNB and MeNB

Without loss of generality, we carry out our analysis considering a typical user located at the origin. We assume that this user operates relatively closer to its home SCeNB. The interfering SCeNBs are distributed according to a PPP ϕ_S with intensity λ_S, independent of ϕ_M. Finally, the MeNBs are distributed according to a homogeneous Poisson point process (PPP) ϕ_M with intensity λ_M. According to strength of the reference signal received power, a user can be associated to either its home SCeNB or the strongest MeNB sector.

We also assume that a time-domain inter-cell interference co-ordination (ICIC) scheme is implemented to avoid excessive interference between neighboring MeNBs, as e.g., in [8]. As a result of this ICIC scheme, we can ignore the interference in the macro tier from the neighboring MeNBs, which is more realistic in dense deployment of small cells and is not a significant omission of interference effects [2].

Hypothesis 1: With the assumptions of closed access SCeNBs and ICIC between MeNBs, the aggregate powers received from the interfering SCeNBs, the home SCeNB, and the MeNB are mutually independent of each other.

B. Bounded Path-Loss Model

In literature, a model with a path-loss coefficient and exponent is generally considered as given below:

$$l(x, y) = C_0||x - y||^{-\alpha}, \tag{1}$$

where x is the location of the transmitter and y is the location of the receiver. Assuming that the receiver is located at the origin and unit coefficient, we have: $l(x) = ||x||^{-\alpha}$. To alleviate the problem of the singularity at origin (the case where the transmitter and receiver are co-located), a bounded path-loss model is adopted as given below:

$$l(x) = \min(1, ||x||^{-\alpha}) \tag{2}$$

This essentially means that the signal from any transmitter located inside a radius of 1 meter from the receiver, does not suffer from path-loss and the signal reception is with unit gain.

C. Shadowing, Fast Fading, and Noise

We assume that the powers received from a SCeNB located in x_i and from the strongest MeNB at the user of interest suffers from shadowing, modeled as independent log-normal random variables, S_{x_i} and S_M respectively. Random variables S_{x_i} and S_{x_j} for $x_i \neq x_j$ are independent and identically distributed with location and scale parameters μ_S and σ_S respectively. The random variable S_M is supposed to have location and scale parameters μ_M and σ_M, respectively. Fast fading power between a transmitter and a receiver is modeled as an exponential random variable h with average power β_h. Furthermore the noise is assumed to be additive white Gaussian with zero mean and variance σ_n^2.

D. Downlink Received Power

As we assume that the user is operating near its home SCeNB, we model the distance between the user and its home SCeNB according to an exponential random variable with probability density function (pdf):

$$f_d(d) = \mu \cdot e^{-\mu d}, \quad \mu \geq 0. \tag{3}$$

The received power at the user from a transmitting eNode-B located at y with transmit power P_y is given by:

$$R = P_y \cdot l(y) \cdot S_y \cdot h_y,$$

where S_y and h_y are respectively the shadowing and fast fading experienced by the signal. Therefore, from the point of view of a typical user, located at origin, the received powers the macro cell, the interfering small cells, and the home SCeNB are respectively given by:

$$R_M = P_M \cdot l(x_M) \cdot S_M \cdot h_M, \tag{4}$$

$$R_S = P_S \sum_{x_i \in \phi_S} S_{x_i} \cdot l(x_i) \cdot h_{x_i}, \tag{5}$$

$$R_H = P_S \cdot S_S \cdot l(d) \cdot h_d. \tag{6}$$

III. Cell Association

In order to take the effect of shadowing into consideration for cell association, the MeNB process is modified into a one dimensional process named as path-loss process with shadowing (PLPS) [8] given by:

$$\tilde{\phi}_M = \{\xi_{Mi} = \frac{||x_i||^\alpha}{S_{x_i}} : x_i \in \phi_M\}. \quad (7)$$

In this one dimensional process, the nearest point to the origin represents the MeNB with the strongest downlink power. The pdf of this point is given by [8]:

$$f_{\xi_{M1}}(x) = \frac{2D}{\alpha} x^{\frac{2}{\alpha}-1} \exp\left(-Dx^{\frac{2}{\alpha}}\right), \quad (8)$$

where $D = \pi\lambda_M \mathbb{E}\left[S_M^{\frac{2}{\alpha}}\right]$.

Lemma 1: The probabilities of the association of the user with the home SCeNB and MeNB are given by:

$$\mathbb{P}_S = \mathbb{E}_{S_S}\left[e^{\frac{A^2}{4B}} \frac{A\sqrt{\pi}}{2\sqrt{B}} erfc\left(\frac{A}{2\sqrt{D}}\right)\right], \quad (11)$$

$$\mathbb{P}_M = 1 - \mathbb{P}_S, \quad (12)$$

where $erfc(.)$ is the complementary error function. $A = \mu\left(\frac{P_M}{P_S S_S}\right)^{-\frac{1}{\alpha}}$ and $D = \lambda_M \pi \mathbb{E}\left[S_M^{\frac{2}{\alpha}}\right]$.

Proof. The user associates with its home SCeNB if the associated received power is greater than that one received from the strongest MeNB. Given that the user is at a distance d from its home SCeNB, the probability of association with home SCeNB is given by:

$$\begin{aligned}\mathbb{P}_S &= \mathbb{P}\left(P_S d^{-\alpha} S_S > P_M \xi_{M1}^{-1}\right) \\ &= \mathbb{P}\left(d < \left(\frac{P_M}{P_S S_S}\right)^{-\frac{1}{\alpha}} \xi_{M1}^{\frac{1}{\alpha}}\right) \\ &\overset{a}{=} 1 - \mathbb{E}_{S_S}\mathbb{E}_{S_M}\mathbb{E}_{\xi_{M1}}\left[e^{-\mu C \xi_{M1}^{\frac{1}{\alpha}}}\right], \quad (13)\end{aligned}$$

where $C = \left(\frac{P_M}{P_S S_S}\right)^{-\frac{1}{\alpha}}$ and the step a is from Eq. (3). Using the pdf of ξ_{M1} and writing $x = \xi_{M1}$, we have:

$$\mathbb{P}_S = 1 - \frac{\mathbb{E}\left[S_M^{\frac{2}{\alpha}}\right] 2\pi\lambda_M}{\alpha} \mathbb{E}_{S_S}\left[\int_0^\infty x^{\frac{2}{\alpha}-1} e^{-\mu C x^{\frac{1}{\alpha}}} e^{-\lambda_M \pi \mathbb{E}[S_M^{\frac{2}{\alpha}}] x^{\frac{2}{\alpha}}} dx\right].$$

Denoting $\mu C = A$ and $\frac{1}{\alpha} = k$, we have:

$$1 - 2\mathbb{E}_{S_S}\left[Dk \int_0^\infty x^{2k-1} e^{-\left(\sqrt{D}x^k + \frac{A}{2\sqrt{D}}\right)^2} e^{\frac{A^2}{4D}} dx\right]. \quad (14)$$

Substituting $\left(\sqrt{D}x^k + \frac{A}{2\sqrt{D}}\right) = t$ and solving the integral, we derive the expression for $\mathbb{P}_S$. □

IV. Average SINR

The instantaneous SINRs experienced by user associated either with the home SCeNB or the MeNB, are now given by:

$$SINR_S = \frac{R_H}{R_M + R_S + \sigma_N^2}, \quad (15)$$

$$SINR_M = \frac{R_M}{R_S + R_H + \sigma_N^2}. \quad (16)$$

According to *Hypothesis 1*, all the terms of Eqs (4), (5), and (6) are independent. The expressions (15) and (16) can be computed as follows:

$$\mathbb{E}[SINR_S] = \mathbb{E}[R_H]\mathbb{E}\left[\frac{1}{R_M + R_S + \sigma_N^2}\right], \quad (17)$$

$$\mathbb{E}[SINR_M] = \mathbb{E}[R_M]\mathbb{E}\left[\frac{1}{R_S + R_H + \sigma_N^2}\right]. \quad (18)$$

To obtain the final derivations of the average SINR, we provide the following useful lemma.

Lemma 2: For a random variable X,

$$\mathbb{E}\left[\frac{1}{X}\right] \approx \frac{1}{\mathbb{E}[X]} + \frac{1}{\mathbb{E}[X]^3} Var(X). \quad (19)$$

Proof. Using the Taylor expansion of $\mathbb{E}\left[\frac{1}{X}\right]$ around $\mathbb{E}[X]$ we have:

$$\begin{aligned}\mathbb{E}\left[\frac{1}{X}\right] &\approx \frac{1}{\mathbb{E}[X]} - \frac{1}{\mathbb{E}[X]^2}\mathbb{E}[(X - \mathbb{E}[X])] \\ &+ \frac{1}{\mathbb{E}[X]^3}\mathbb{E}[(X - \mathbb{E}[X])^2] \\ &= \frac{1}{\mathbb{E}[X]} + \frac{1}{\mathbb{E}[X]^3} Var(X).\end{aligned}$$

□

Furthermore, we note the following identity that will be used in deriving the final expressions:

Identity 1: The variance of product of n independent random variables is given by:

$$Var(X_1 X_2 \ldots X_n) = \prod_{i=1}^n \left(Var(X_i) + (\mathbb{E}[X_i])^2\right) - \prod_{i=1}^n (\mathbb{E}[X_i])^2. \quad (20)$$

Let's modify the SCeNB process into a 1D processes as:

$$\phi_S' = \{\xi_{Si} = ||x_i||^\alpha : x_i \in \phi_S\}. \quad (21)$$

$$\mathbb{E}[R_M] = P_M\beta_h\left(1 - e^{-\lambda_M\pi\mathbb{E}[S_M^{\frac{2}{\alpha}}]} + (\pi\lambda_M\mathbb{E}[S_M^{\frac{2}{\alpha}}])^{\frac{\alpha}{2}}\Gamma\left(1-\frac{\alpha}{2},\pi\lambda_M\mathbb{E}[S_M^{\frac{2}{\alpha}}]\right)\right) \tag{9}$$

$$Var(R_M) = 2P_M\beta_h^2\left(1 - e^{-\lambda_S\pi\mathbb{E}[S_M^{\frac{2}{\alpha}}]} + (\pi\lambda_M\mathbb{E}[S_M^{\frac{2}{\alpha}}])^{\alpha}\Gamma\left(1-\alpha,\pi\lambda_M\mathbb{E}[S_M^{\frac{2}{\alpha}}]\right)\right) - (\mathbb{E}[R_M])^2 \tag{10}$$

This path-loss process without shadowing is non-homogeneous with intensity measure and intensity given by [9]:

$$\Lambda_S'(r) = \lambda_S\pi r^{\frac{2}{\alpha}},$$
$$\lambda_S'(r) = \frac{d}{dr}\Lambda_S'(r) = \frac{2\pi\lambda_S}{\alpha}r^{\frac{2}{\alpha}-1}. \tag{22}$$

Lemma 3: The mean and variance of R_M of Eq. (4) are given by Eq. (9) and (10).

Proof. R_M is essentially the power from the strongest MeNB ξ_{M1}, the average value of which can be computed as:

$$\mathbb{E}[R_M] = P_M\sum_{i=1}^{3}\mathbb{E}[h_i]\mathbb{E}[\xi_{M1}^{-1}].$$

Now,

$$\mathbb{E}[\xi_{M1}^{-1}] = \int_0^\infty \xi_{M1}^{-1}f_{\xi_{M1}}d\xi_{M1}.$$

Using the values of Eq. (2) and the distribution of ξ_{M1} from Eq. (8), we have:

$$\mathbb{E}[\xi_{M1}^{-1}] = \frac{2\pi\lambda_M\mathbb{E}[S_M^{\frac{2}{\alpha}}]}{\alpha}\int_0^1 \xi_{M1}^{\frac{2}{\alpha}-1}e^{-\lambda_M\pi\mathbb{E}[S_M^{\frac{2}{\alpha}}]\xi_{M1}^{\frac{2}{\alpha}}}d\xi_{M1}$$
$$+\int_1^\infty \frac{2\pi\lambda_M\mathbb{E}[S_M^{\frac{2}{\alpha}}]}{\alpha}\xi_{M1}^{\frac{2}{\alpha}-2}e^{-\lambda_M\pi\mathbb{E}[S_M^{\frac{2}{\alpha}}]\xi_{M1}^{\frac{2}{\alpha}}}d\xi_{M1} \tag{23}$$

and

$$Var(\xi_{M1}^{-1}) = \mathbb{E}[\xi_{M1}^{-2}] - \mathbb{E}[\xi_{M1}^{-1}]^2, \tag{24}$$

where

$$\mathbb{E}[\xi_{M1}^{-2}] = \int_0^\infty \xi_{M1}^{-2}f_{\xi_{M1}}d\xi_{M1}$$
$$= \frac{2\pi\lambda_M\mathbb{E}[S_M^{\frac{2}{\alpha}}]}{\alpha}\int_0^1 \xi_{M1}^{\frac{2}{\alpha}-1}e^{-\lambda_M\pi\mathbb{E}[S_M^{\frac{2}{\alpha}}]\xi_{M1}^{\frac{2}{\alpha}}}d\xi_{M1}$$
$$+\int_1^\infty \frac{2\pi\lambda_M\mathbb{E}[S_M^{\frac{2}{\alpha}}]}{\alpha}\xi_{M1}^{\frac{2}{\alpha}-3}e^{-\lambda_M\pi\mathbb{E}[S_M^{\frac{2}{\alpha}}]\xi_{M1}^{\frac{2}{\alpha}}}d\xi_{M1}. \tag{25}$$

Solving Eq. (23) and substituting in Eq. (24) and using Eq. (25) we get $Var(\xi_{M1}^{-1})$. The variance of the received power from the MeNB is calculated using Eq. (20) for the case $n = 2$ with $X_1 = \xi_{M1}^{-1}$ and $X_2 = h_M$. □

Now, the instantaneous aggregate interference from the small cell tier is given by R_S in Eq. (5).

Let $G_S = \sum_{x\in\phi_S} l(x)$.

Lemma 4: The mean and variance of G_S are given by:

$$\mathbb{E}[G_S] = \pi\lambda_S + \frac{2\pi\lambda_S}{\alpha-2}, \tag{30}$$

$$Var(G_S) = \pi\lambda_S + \frac{\pi\lambda_S}{\alpha-1}. \tag{31}$$

Proof. Using Eq. (21), Eq. (2), and the Campbell's theorem [9], we can write:

$$\mathbb{E}[G_S] = \mathbb{E}\left[\sum_{x_i\in\phi_S} l(x_i)\right]$$
$$= \int_0^1 \lambda_S'(\xi_S)d\xi_S + \int_1^\infty \xi_S^{-1}\lambda_S'(\xi_S)d\xi_S \tag{32}$$

$$Var(G_S) = \mathbb{E}[G_S^2] - \mathbb{E}[G_S]^2, \tag{33}$$

$$\mathbb{E}[G_S^2] = \mathbb{E}\left[\left(\sum_{x_i\in\phi_S} l(x_i)\right)^2\right]$$
$$= \mathbb{E}\left[\sum_{x_i\in\phi_S} l(x_i)^2\right] + \mathbb{E}\left[\sum_{x_i,x_j\in\phi_S}^{\neq} l(x_i)l(x_j)\right], \tag{34}$$

where the $\neq$ denotes that the points x_i and x_j are distinct. Now,

$$\mathbb{E}\left[\sum_{x_i,x_j\in\phi_S}^{\neq} l(x_i)l(x_j)\right]$$
$$= \int_{\mathbb{R}}\int_{\mathbb{R}} l(x_i)l(x_j)\lambda_S'(x_i^{-1})\lambda_S'(x_j^{-1})dx_idx_j$$
$$= (\mathbb{E}[G_S])^2. \tag{35}$$

$$\mathbb{E}[R_S] = \beta_h P_S \left(e^{\mu_S + \frac{\sigma_S^2}{2}}\right)\left(\pi\lambda_s + \frac{2\pi\lambda_S}{\alpha-2}\right) \tag{26}$$

$$Var(R_S) = 2P_S^2\beta_h^2(e^{2\mu_S\sigma_S^2+\sigma_S^4})\left(2\pi\lambda_S + \frac{\pi\lambda_S}{\alpha-1} + \frac{2\pi\lambda_S}{\alpha-2}\right) - (\mathbb{E}[R_S])^2 \tag{27}$$

$$\mathbb{E}[R_H] = \beta_h P_S \left(e^{\mu_S + \frac{\sigma_S^2}{2}}\right)\left(1 - e^{-\mu} + \mu^\alpha\Gamma(1-\alpha,\mu)\right) \tag{28}$$

$$Var(R_H) = 2P_S^2\beta_h^2(e^{2\mu_S\sigma_S^2+\sigma_S^4})\left(1 - e^{-\mu} + \mu^{2\alpha}\Gamma(1-2\alpha,\mu)\right) - (\mathbb{E}[R_H])^2 \tag{29}$$

Thus,

$$Var(G_S) = \mathbb{E}\left[\sum_{x_i\in\phi_S} l(x_i)^2\right] \tag{36}$$

$$= \int_0^1 \lambda'_S(\xi_S)d\xi_S + \int_1^\infty \xi_S^{-2}\lambda'_S(\xi_S)d\xi_S. \tag{37}$$

Substituting the expression for $\lambda'_S(r)$ from Eq. (22) and solving the integrals completes the proof. □

The mean of the received power from the interfering SCeNBs is given by:

$$\mathbb{E}[R_S] = \mathbb{E}[S_S]\mathbb{E}\left[G_S\right]\mathbb{E}[h_S]P_S,$$

which can be calculated using Eq. (30) and is given by Eq. (26). The variance of the received power from the small cell BS (i.e., $Var(R_S)$) is calculated using Eq. (20) for the case $n = 3$ with $X_1 = S_S, X_2 = G_S$ and $X_3 = h_S$ and is given by Eq. (27).

Let's recall that the instantaneous received power from the home SCeNB is given by Eq. (6) and define $G_H = l(d)$.

Lemma 5: The mean and variance of G_H are given by:

$$\mathbb{E}[G_H] = 1 - e^{-\mu} + \mu^\alpha\Gamma(1-\alpha,\mu), \tag{39}$$

$$Var(G_H) = 1 - e^{-\mu} + \mu^{2\alpha}\Gamma(1-2\alpha,\mu) - (\mathbb{E}[G_H])^2. \tag{40}$$

Proof. Since the distance between the user and the home SCeNB is exponentially distributed as given by Eq. (3), we have:

$$\mathbb{E}[G_H] = \int_0^\infty l(r)f_r(r)dr$$

$$= \int_0^1 \mu e^{-\mu r}dr + \int_1^\infty r^{-\alpha}\mu e^{-\mu r}dr$$

Using Eq. (2) and Eq. (3) in the above equation, the mean is obtained. Similarly carrying out the same calculations in the following:

$$Var(G_H) = \mathbb{E}[G_H^2] - (\mathbb{E}[G_H])^2$$

$$= \int_0^1 \mu e^{-\mu r}dr + \int_1^\infty r^{-2\alpha}\mu e^{-\mu r}dr,$$

the variance is obtained. □

The mean of the received power from the home SCeNB R_H is given by:

$$\mathbb{E}[R_H] = \mathbb{E}[S_S]\mathbb{E}\left[G_H\right]\mathbb{E}[h_S]P_S.$$

The variance of R_H ($Var(R_H)$) is calculated using Eq. (20) for the case $n = 3$ with $X_1 = S_S, X_2 = G_H$ and $X_3 = h_d$. The final values of $\mathbb{E}[R_H]$ and $Var(R_H)$ are given by Eq. (28) and Eq. (29).

Theorem 1: The approximate value of expected SINR of the network is given by Eq. (38).

Proof. Given the user is associated with the home small cell eNode-B, the expected value of the SINR is given by Eq. (15). Using *Lemma 2*, we have:

$$\mathbb{E}[SINR_S] = \mathbb{E}\left[R_H\right]\mathbb{E}\left[\frac{1}{R_M + R_S + N}\right]$$

$$\approx \mathbb{E}\left[R_H\right]\left[\frac{1}{\mathbb{E}[R_M + R_S + N]}\right]$$

$$+ \mathbb{E}\left[R_H\right]\left[\frac{Var(R_M + R_S + N)}{\mathbb{E}[R_M + R_S + N]^3}\right]. \tag{41}$$

Following the same approach as described for the home SCeNB association case, the approximate value of the expected SINR in case of association with MeNB can be calculated. Finally, the expected value of the SINR of the network is given by:

$$\mathbb{E}[SINR] = \mathbb{P}_S\mathbb{E}[SINR_S] + (1-\mathbb{P}_S)\mathbb{E}[SINR_M] \tag{42}$$

□

$$\mathbb{E}[SINR] = \mathbb{P}_S \mathbb{E}[R_H] \left[\frac{1}{\mathbb{E}[R_M] + \mathbb{E}[R_S] + \sigma_N^2} + \frac{Var(R_M) + Var(R_S)}{(\mathbb{E}[R_M] + \mathbb{E}[R_S] + \sigma_N^2)^3} \right] + (1 - \mathbb{P}_S)\mathbb{E}[R_M] \left[\frac{1}{\mathbb{E}[R_S] + \mathbb{E}[I_H] + \sigma_N^2} + \frac{Var(R_H) + Var(R_S)}{(\mathbb{E}[R_H] + \mathbb{E}[R_S] + \sigma_N^2)^3} \right] \quad (38)$$

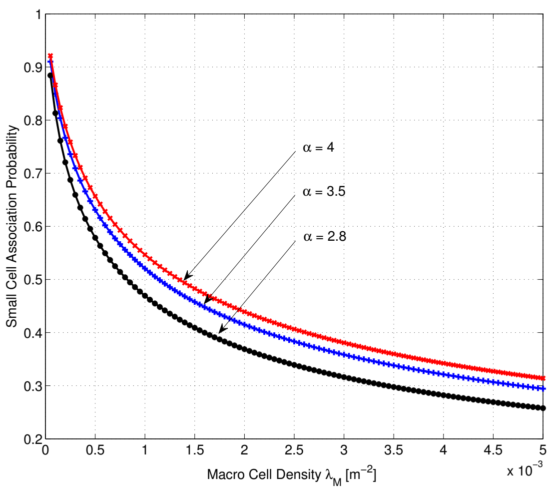

Fig. 2. Small cell association probability vs. MeNB density.

V. Average Downlink Spectral Efficiency

In this section we use the derived approximations for the average SINR to come up with approximations for the average downlink spectral efficiency of the network. We will first obtain an upper bound on the average downlink spectral efficiency and then provide an approximation which turns out to be tight in the considered scenario.

Theorem 2: The upper bound of the average spectral efficiency of the network is given by $\log_2(1+\mathbb{E}[SINR])$ where $\mathbb{E}[SINR]$ is obtained from *Theorem 1*.

Proof. The spectral efficiency of the network is given by:

$$\mathcal{R} = \log_2(1 + SINR). \quad (43)$$

Using Jensen's inequality, the expected value of spectral efficiency can be upper bounded as:

$$\mathbb{E}[\mathcal{R}] = \mathbb{E}[\log_2(1 + SINR)] \leq \log_2(1 + \mathbb{E}[SINR]). \quad (44)$$

Substituting the value of $\mathbb{E}[SINR]$ from Eq. (38), completes the proof. □

TABLE I
SIMULATION PARAMETERS

Parameter	Value	Parameter	Value
P_M	15 dBW	P_S	5 dBW
σ_S^2	6 dB	σ_M^2	6 dB
μ_M	0 dB	μ_S	0 dB
μ	0.1 m^{-1}	N_0	-174dBm/Hz
β_h	0 dB	B	10 MHz
σ_N^2	$N_0 \cdot B$		

VI. Simulation Results

In this section we validate the theoretical results obtained using extensive Monte-Carlo simulations. The simulation parameters are given in Table. I. The probability of association with the home SCeNB given by Eq. (12) is shown as a function of MeNB density in Fig. 2. The association probability decreases with increasing λ_M as expected. Also it can be noted that the association probability with the home SCeNB increases with increasing α for the same value of MeNB density. This is because, as the user operates relatively closer to the home SCeNB as compared to the MeNB, a higher path-loss exponent reduces the received power from MeNB more than it reduces the received power from home SCeNB.

In Fig. 3(a) and 3(b) we compare the approximated value of the average SINR derived in Eq. (38) to the actual SINR evaluated by simulations, for different shadowing scale parameter and with $\lambda_M = 5e-05m^{-2}$. We notice that in both cases, for $\alpha = 2.8$, the approximation is quite accurate for higher values of λ_S i.e., for dense deployment of SCeNBs. As the value of α is increased, the approximation becomes more accurate for lower values of λ_S. We can also observe that the average SINR at the user increases with increasing α. This is because, with increasing α, the user has more probability of associating with the home SCeNB, which provides higher power to the user being closer as compared to MeNB which is comparatively farther.

In Fig. 4(a) and 4(b) we compare the upper bound on the average spectral efficiency derived in Eq. (44) to the numerical results obtained by simulations for different shadowing scale parameters and with $\lambda_M = 5e-05m^{-2}$. For the sake of completeness, the approximation with

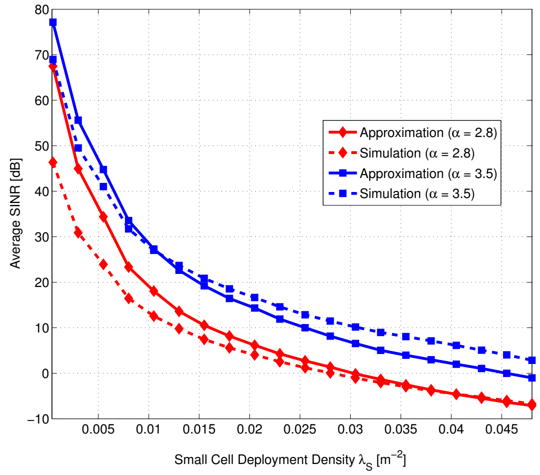

(a) Without shadowing $\sigma_S^2 = 0$ dB and $\sigma_M^2 = 0$ dB.

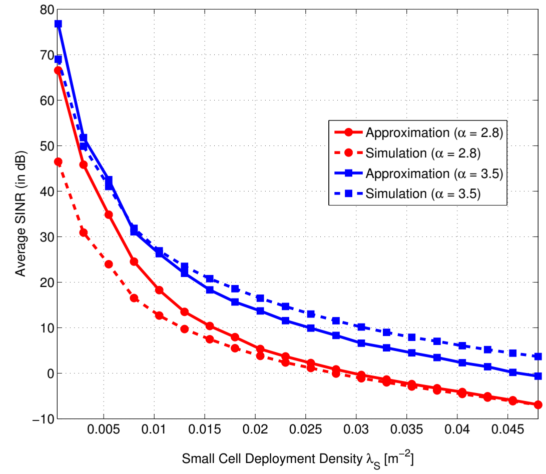

(b) With shadowing $\sigma_S^2 = 6$ dB and $\sigma_M^2 = 6$ dB.

Fig. 3. Average SINR vs small cell deployment density.

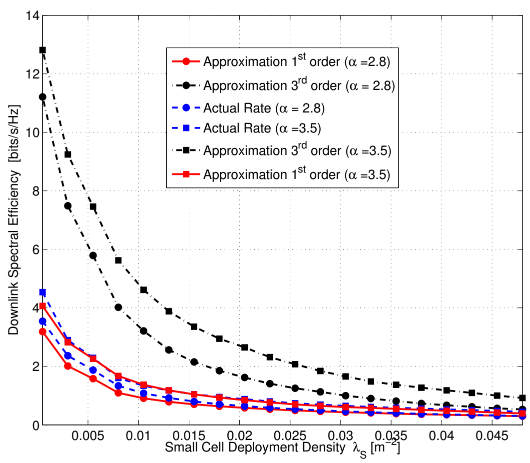

(a) Without shadowing $\sigma_S^2 = 0$ dB and $\sigma_M^2 = 0$ dB.

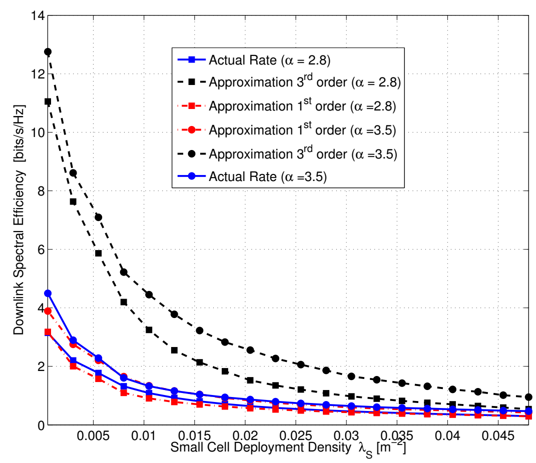

(b) With shadowing $\sigma_S^2 = 6$ dB and $\sigma_M^2 = 6$ dB.

Fig. 4. Average spectral efficiency and spectral efficiency bound vs. small cell deployment density.

first order of the Taylor expansion is also shown. First, it can be observed that the shadowing values do not effect the tightness of the bound. Second, the bound becomes tighter at higher values of λ_S. Finally, we can see that the first order approximation of the Taylor series gives a tighter estimation as compared to the upper bound in the ranges of λ_S under study. This is due to the fact that, the following two opposite inequalities compete to give an approximation:

$$\mathbb{E}[\log_2(1 + SINR)] \leq \log_2(1 + \mathbb{E}[SINR]) \geq \log_2\left(1 + \mathbb{E}[S]\frac{1}{\mathbb{E}[I+\sigma_N^2]}\right), \qquad (45)$$

where S represents the signal and I represents the interference in different cases. However, we cannot guarantee that the approximation provided by the first order of the Taylor series is always tighter as compared to the derived upper bound as quantifying the opposite inequalities is not straightforward.

VII. Conclusion

In this paper, we have analysed the performance of HetNets with closed access small cells complementing the macro tier eNodeBs by using tools from stochastic geometry. The analysis is carried out in a simpler way as compared to that existing in the literature. We have derived the expression for probability of association of a user with the home SCeNB and with the MeNB. We have derived expressions for approximating the average downlink spectral efficiency as perceived by the user. This is then used to derive upper bounds on the achievable downlink spectral efficiency of the network. Using only the first order approximation of the Taylor's series, very accurate approximations are obtained for the scenario under consideration. In addition to provide a reliable and simple tool to characterize the performance evaluation, the obtained results can be used for optimized network planning and adaptive interference coordination mechanisms.

VIII. ACKNOWLEDGMENT

This work has been partially performed in the framework of the Horizon 2020 project FANTASTIC-5G (ICT-671660) receiving funds from the European Union. The authors would like to acknowledge the contributions of their colleagues in the project, although the views expressed in this contribution are those of the authors and do not necessarily represent the project.

References

[1] D. López-Pérez, M. Ding, H. Claussen, and A. H. Jafari. Towards 1 gbps/ue in cellular systems: understanding ultra-dense small cell deployments. *IEEE Communications Surveys & Tutorials*, 17(4):2078–2101, 2015.

[2] H. S. Jo, P. Xia, and J. G. Andrews. Open, closed, and shared access femtocells in the downlink. *EURASIP Journal on Wireless Communications and Networking*, 2012(1):1–16, 2012.

[3] T. QS Quek, G. de la Roche, İ. Güvenç, and M. Kountouris. *Small cell networks: Deployment, PHY techniques, and resource management*. Cambridge University Press, 2013.

[4] H. ElSawy, E. Hossain, and M. Haenggi. Stochastic geometry for modeling, analysis, and design of multi-tier and cognitive cellular wireless networks: A survey. *IEEE Communications Surveys & Tutorials*, 15(3):996–1019, 2013.

[5] T. Bai and R. W. Heath. Coverage and rate analysis for millimeter-wave cellular networks. *IEEE Transactions on Wireless Communications,*, 14(2):1100–1114, 2015.

[6] M. Di Renzo, A. Guidotti, and G. E. Corazza. Average rate of downlink heterogeneous cellular networks over generalized fading channels: a stochastic geometry approach. *IEEE Transactions on Communications,*, 61(7):3050–3071, 2013.

[7] Y. J. Chun, M. O Hasna, and A. Ghrayeb. Modeling heterogeneous cellular networks interference using poisson cluster processes. *IEEE Journal on Selected Areas in Communications,*, 33(10):2182–2195, 2015.

[8] X. Zhang and M. Haenggi. A stochastic geometry analysis of inter-cell interference coordination and intra-cell diversity. *IEEE Transactions on Wireless Communications,*, 13(12):6655–6669, 2014.

[9] M. Haenggi. *Stochastic geometry for wireless networks*. Cambridge University Press, 2012.